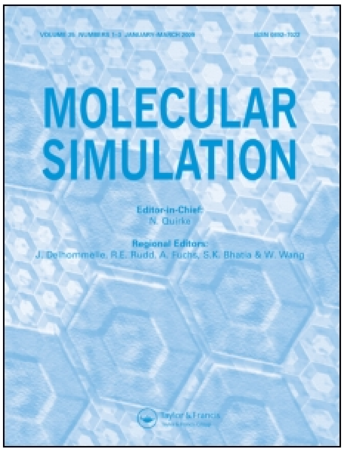

Molecular Simulation

Publication details, including instructions for authors and subscription information:
http://www.informaworld.com/smpp/title~content=t713644482

An Efficient Way to Conserve the Total Energy in Molecular Dynamics Simulations; Boundary Effects on Energy Conservation and Dynamic Properties

Olle Teleman[a]
[a] Dept. of Physical Chemistry 2, Chemical Centre, Lund, Sweden

To cite this Article Teleman, Olle(1988) 'An Efficient Way to Conserve the Total Energy in Molecular Dynamics Simulations; Boundary Effects on Energy Conservation and Dynamic Properties', Molecular Simulation, 1: 5, 345 — 355
To link to this Article: DOI: 10.1080/08927028808080956
URL: http://dx.doi.org/10.1080/08927028808080956

Molecular Simulation, 1988, Vol. 1, pp. 345–355
Photocopying permitted by license only
Reprints available directly from the publisher

AN EFFICIENT WAY TO CONSERVE THE TOTAL ENERGY IN MOLECULAR DYNAMICS SIMULATIONS; BOUNDARY EFFECTS ON ENERGY CONSERVATION AND DYNAMIC PROPERTIES

OLLE TELEMAN

Dept. of Physical Chemistry 2, Chemical Centre, POB 124, S-221 00 Lund, Sweden

(*Received October 1987, in final form March 1988*)

Molecular Dynamics simulations of pure water are reported, where the so-called jump correction i.e., inclusion of the Dirac delta force corresponding to the potential discontinuity at cutoff, ensures that the force is the negative gradient of the potential everywhere. Results are compared to those obtained for potentials truncated in the ordinary way and for potentials where the discontinuity is removed by means of a switching function. The jump correction and the switching functions provide excellent conservation of the total energy, and remove the need for temperature scaling at equilibrium. Radial distributions are insensitive to boundary conditions. Translational and rotational diffusion vary considerably with boundary conditions and also with cutoff distance.

KEY WORDS: Molecular Dynamics simulation, potential boundary, water, energy conservation, radial distributions, translational diffusion.

INTRODUCTION

Molecular dynamics simulations are normally subject to several assumptions and numerical constraints. One constraint is that the integration algorithm puts a limit to the time step. Other assumptions are that the potential is pairwise additive and that a small sample with periodic boundary conditions will reproduce macroscopic properties. The size of the simulated sample is closely related to the boundary conditions, which are in turn related to the long range behaviour of the potential, which is very long ranged for charged and dipolar systems.

Several approaches have been made to the treatment of the long range part of the potential. Lado used integral equations (applying the reference hypernetted chain closure) to treat the environment of the explicitly simulated sample [1]. This technique is limited to a few special cases as yet. With periodic boundary conditions we may treat the entire crystal correctly by Ewald summation [2], or we may treat the environment as a dielectric continuum by including the so called reaction field [3]. These last two treatments are physically not fully accurate, as the environment, in reality, is neither crystal-like nor completely uncorrelated.

As regards the functional form of the explicitly evaluated potential it is common practise to truncate it at a certain distance r_{cut}. This amounts to a potential discontinuity, while most algorithms require force and potential to be continuous. One suggestion is to shift the potential to make it zero at cutoff [4], but this does not remove the discontinuity in the force. Another is to apply a switching function, which smoothly brings the potential down to zero over some distance [5]. If one does not want to compromise on the potential function inside the cutoff one has to include a further border region in the interaction volume. This increases the amount of computation substantially (with 10 Å to 11 Å, by 33 per cent!). Rather, we will here investigate the correct integration of the potential with the discontinuity by including the corresponding Dirac delta force.

THEORY AND METHODOLOGY

The starting point for the present simulations is the straightforward spherical cutoff. This is employed in an MD program described elsewhere [6], which was used to generate reference trajectories.

The Jump Correction.

The spherical cutoff amounts to a potential discontinuity, which the integration algorithm cannot handle properly, but which can be treated in the following way. The force on a particle is obtained as the gradient of the potential with respect to its position. The derivative of the barrier is a Dirac delta function, the effect of which is to alter the velocity of the particle instantaneously. Let two particles approach each other, *cf.* Figure. 1a. At time t = 0 the distance between them is D, which is the distance inside which they interact, cf. Figure 1b. When the distance is between D and D-d a force acts on the particles (x is the position, v the velocity and m refers to the mass of each particle):

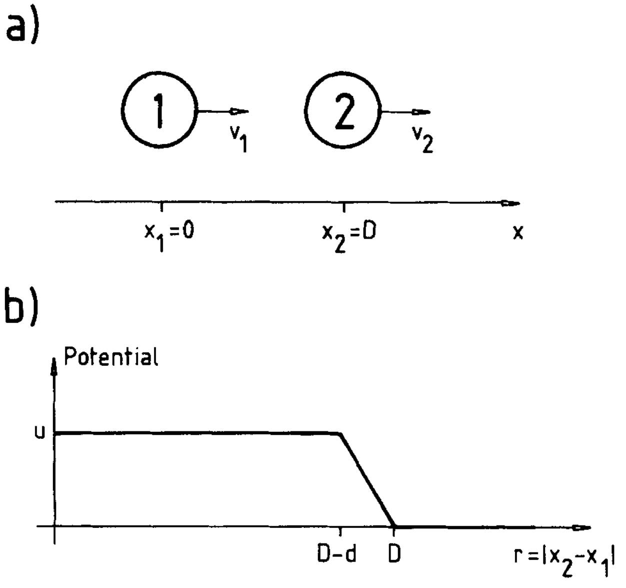

Figure 1 Notation a) Two particles at time $t = 0$, x is the position, v the velocity and their masses are m_1 and m_2. b) The interparticle potential energy, where r is the distance between particles 1 and 2.

$$\frac{d^2x_1}{dt^2} = -\frac{u}{m_1 d}, \quad \frac{d^2x_2}{dt^2} = \frac{u}{m_2 d} \tag{1}$$

and, by integration.

$$\frac{dx_1}{dt} = v_1 - \frac{u}{m_1 d}t, \quad \frac{dx_2}{dt} = v_2 + \frac{u}{m_2 d}t \tag{2}$$

and

$$x_1 = 0 + v_1 t - \frac{u}{2m_1 d}t^2, \; x_2 = D + v_2 t + \frac{u}{2m_2 d}t^2 \tag{3},$$

where we use the boundary conditions

$$x_1(0) = 0, \; x_2(0) = D, \; \left.\frac{dx_1}{dt}\right|_{t=0} = v_1, \; \left.\frac{dx_2}{dt}\right|_{t=0} = v_2 \tag{4}$$

with $v_1 > v_2$ and $D > 0$. The barrier is successfully scaled if the distance between particles, $x_2 - x_1$, reaches $D-d$ at some time t, that is, if

$$x_2 - x_1 = D + (v_2 - v_1)\,t + \frac{u}{2d}\left[\frac{1}{m_1} + \frac{1}{m_2}\right]t^2 = D - d \tag{5}.$$

This gives

$$t = -\frac{\mu d}{u}(v_2 - v_1)\,(\pm)\,\frac{\mu d}{u}\left[(v_2 - v_1)^2 - \frac{2u}{\mu}\right]^{0.5} \tag{6}$$

with

$$\mu = \frac{m_1 m_2}{m_1 + m_2} \tag{7}.$$

The solutions to equation (5) are real if

$$\tfrac{1}{2}\mu(v_2 - v_1)^2 \geqslant u \tag{8},$$

which is the energetic criterion for passing the barrier. Equations (3) and (6) then give the final velocities:

$$\begin{cases} \dfrac{dx_1}{dt} = p_1 v_1 + p_2\left[v_2 + \left[(v_2 - v_1)^2 - \dfrac{2u}{\mu}\right]^{0.5}\right] \\ \dfrac{dx_2}{dt} = p_2 v_2 + p_1\left[v_1 - \left[(v_2 - v_1)^2 - \dfrac{2u}{\mu}\right]^{0.5}\right] \end{cases} \tag{9}$$

where $p_1 = m_1/(m_1 + m_2)$ and $p_2 = m_2/(m_1 + m_2)$. If the particles start inside the interaction volume and withdraw from each other ($v_2 > v_1$), we get

$$\begin{cases} \dfrac{dx_1}{dt} = p_1 v_1 + p_2\left[v_2 - \left[(v_2 - v_1)^2 + \dfrac{2u}{\mu}\right]^{0.5}\right] \\ \dfrac{dx_2}{dt} = p_2 v_2 + p_1\left[v_1 + \left[(v_2 - v_1)^2 + \dfrac{2u}{\mu}\right]^{0.5}\right] \end{cases} \tag{10},$$

and the counterpart of relation (8) is

$$\tfrac{1}{2}\mu(v_2 - v_1)^2 \geqslant -u \tag{11}$$

The limit of infinite steepness (d → 0) is trivial as *d* does not appear in Equations (9) and (10). If relation (8) (or (11)) is not satisfied, the particles rebound elastically. Final velocities are then obtained from the positive (later) time at which $x_2 - x_1 = D$:

$$t = -\frac{2\mu d}{u}(v_2 - v_1) \qquad (\text{or } t = 0) \tag{12}$$

and

$$\begin{cases} \dfrac{dx_1}{dt} = v_1 + 2p_2(v_2 - v_1) \\[2ex] \dfrac{dx_2}{dt} = v_2 + 2p_1(v_2 - v_1) \end{cases} \tag{13}$$

The application of Equations (8) – (13) in a molecular dynamics simulation will be referred to as the jump correction.

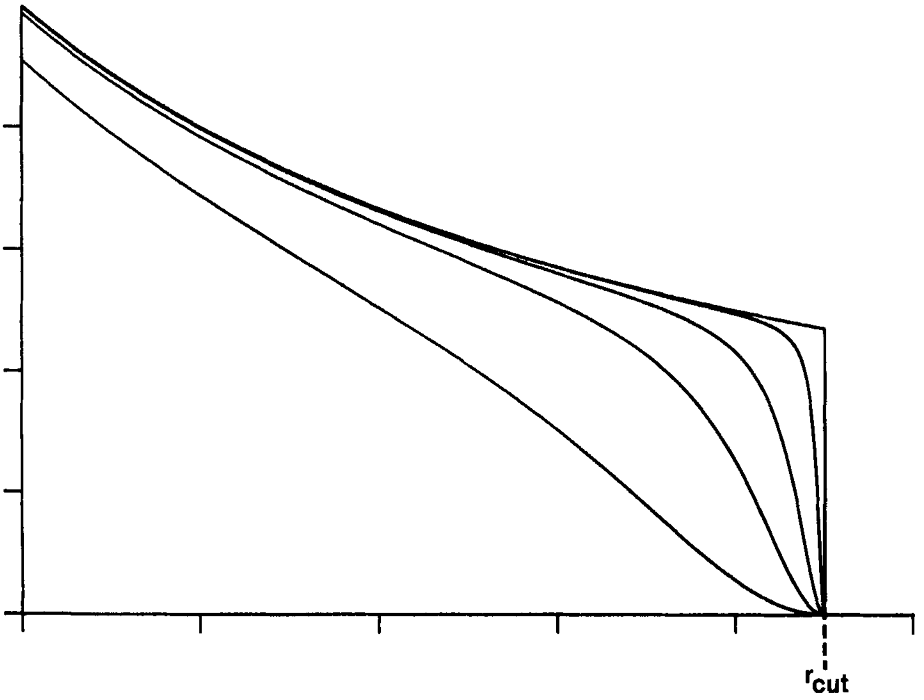

Figure 2 The coulomb potential close to the cutoff (top curve), and the coulomb potential multipled by a switching function (see equation (14)) with c = 2, 0.25, 0.04, and 0.0025 Å^2 (second to fifth curves from top). Arbitrary units on the ordinate, on the abscissa one division corresponds to 1 Å.

The Switching Function

The switching function used has the form

$$s(r) = \frac{(r - r_{\text{cut}})^2}{(r - r_{\text{cut}})^2 + c} \tag{14},$$

where the choice of c determines the steepness of the switch. The effect of a switching function on a Coulomb potential is shown in Fig. 2. If the cutoff is applied atom by atom, introduction of a switching function is straightforward. In our water simulations, the cutoff is applied molecule by molecule in order not to introduce any artificial net charges, and the switching function has to be treated similarly. If the oxygen-oxygen interaction is modified by a switching function to give $V'(r_{OO}) = V(r_{OO}) \cdot S(r_{OO})$, then $S(r_{OO})$ must be used also for O–H and H–H interactions. More explicitly, let the atoms of two water molecules be numbered from 1 to 3 and 4 to 6, with 1 and 4 being the oxygen atoms. We then have a total potential for the pair of molecules of

$$V' = [V_{14} + V_{15} + V_{16} + V_{24} + V_{25} + V_{26} + V_{34} + V_{35} + V_{36}] \cdot S(r_{14}) \tag{15}$$

which gives a force on atom 1 of

$$\begin{aligned} F_1 = {} & [-\nabla_1 V_{14} - \nabla_1 V_{15} - \nabla_1 V_{16}] \cdot S(r_{14}) \\ & + [V_{14} + V_{15} + V_{16} + V_{24} + V_{25} + V_{26} + V_{34} + V_{35} + V_{36}] \cdot (-\nabla_1 S(r_{14})) \end{aligned} \tag{16}$$

where ∇_1 denotes the gradient with respect to the position of atom 1. A similar expression obtains for atom 4. The force on atom 2 is

$$F_2 = [-\nabla_2 V_{24} - \nabla_2 V_{25} - \nabla_2 V_{26}] \cdot S(r_{14}) \tag{17}$$

with corresponding expressions for atoms 3, 5, and 6. The use of r_{OO} as a basis for the molecular switching function means that the extra terms in the force expressions only appear for the oxygen atoms. This is the procedure followed here. If one uses, say, the distance between centres of mass, the switching function becomes a function of all six atom positions, $S = S(\vec{r}_1, \vec{r}_2, \ldots, \vec{r}_6)$, which implies altogether 36 further terms in Equation (17) and counterparts.

SIMULATIONS PERFORMED

Two pure water systems were simulated, one contained 216 water molecules in a cubic box of side length 18.6 Å and the other contained 1000 water molecules in a box of side length 31.0 Å. The intermolecular potential was the Simple Point Charge (SPC) model [7] and the intramolecular potential was that of reference [6] (for parameter values, see the appendix).

For the smaller system the end point of an earlier 23 picosecond (ps) simulation (similar to those of reference [8]) was used as starting point of seven parallel simulations. The jump correction was used in one (referred to as "*j*8"), a switching function was applied in four ("*s*1", "*s*2", "*s*3" and "*s*4"), the usual spherical cutoff was used in one for purposes of comparison ("*o*8") and the seventh was a cluster simulation ("*c*") where the periodic boundary conditions were removed. For the larger system the end point of an earlier 25 ps simulation was used as a starting point of two parallel

Table 1 Simulation parameters. In all simulations except *c* the neighbour list was updated every 4.8 fs. All trajectories were sampled every 0.096 ps.

Simulation	*Equilibration (ps)*	*Trajectory (ps)*	*Scaling interval (ps)*
*o*8	23. + 8.	38.	0.096
*j*8	23. + 8.	38	1.92
*s*1 ($c = 2$ Å^2)	23. + 10.	15.	0.48
*s*2 ($c = 0.25$ Å^2)	23. + 5.	12.	0.48
*s*3 ($c = 0.04$ Å^2)	23. + 6.	12.	0.48
*s*4 ($c = 0.0025$ Å^2)	23. + 6.	12.	0.48
*o*12	25. + 8.	15.	0.096
*j*12	25. + 8.	15.	0.096
c	23. + 8.	15.	0.096

simulations, one with the jump correction (referred to as "*j*12") and one without ("*o*12"). The cutoff distance was 8.5 Å for the smaller system and 12.0 Å for the larger. For simulation details, see Table 1, and for further information on simulation procedure, see the appendix.

The jump correction (Equations (8)–(13)) was implemented as follows. In a molecular dynamics simulation the potential discontinuity occurs when the neighbour list is updated. When the neighbour list is constructed it is checked for changes and all these are treated according to Equations (8)–(13). Whenever relation (8) or (11), as applicable, is not satisfied, the attempted change in the neighbour list is rejected. The switching function simulations used Equations (14)–(17). The *c* parameter was 2, 0.25, 0.04 and 0.0025 Å^2 in the *s*1, *s*2, *s*3, and *s*4 trajectories respectively, which corresponds to $s(r) = 0.5$ at 1.41, 0.5, 0.2 and 0.05 Å inside the cutoff.

RESULTS AND DISCUSSION

In a simulation where the temperature is scaled, the total energy is not a constant of motion. The ith time the temperature is scaled, the energy of the system is changed by S_i, so that $E_i = E_{i-1} + S_i$. The conserved property is

$$E_i' = E_i - \sum_{j=1}^{i} S_j \tag{18),}$$

which is the total energy corrected for the energy artificially added or removed. Table 2 gives the relative drift in E_i' for all nine trajectories as well as simulation averages. For the small and large systems the jump correction reduces the energy drift by approximate factors of 320 and 140 respectively and the remaining energy variation appears more or less stochastic. The drift in total energy is, in fact, small enough that a 100 ps simulation may be performed without any temperature scaling at all. The jump correction is thus a way to implement the pure microcanonical ensemble in simulations with truncated potentials. For the smaller system, the switching function reduces the drift in energy by about a factor of 180 in the present implementation. That the energy conservation is not quite as good as with the jump correction is because an approaching molecule is detected only some distance δ inside the cutoff. Typically, $\delta = 0.02$ Å with the used neighbour list update interval, and at $r = r_{\text{cut}} - \delta$ $V_{\text{ij}}' = V_{\text{ij}} \cdot S_{\text{ij}}$ already has a nonzero value, so that in practise a small discontinuity

Table 2 Simulation averages. The somewhat lesser cpu consumption for the *s* simulations as compared to *j*8 and *o*8 is the result of using a specialized interaction routine written to accommodate the switching function, whereas otherwise the fully general program was used.

Simulation	*Total energy (kJ/mol)*	*Relative energy drift* (ps^{1})	*Potential energy (kJ/mol)*
*o*8	−28.8 ± 0.2	$-4.5 \cdot 10^{-2}$	−40.2 ± 0.2
*j*8	−30.1 ± 0.2	$1.4 \cdot 10^{-4}$	−41.3 ± 0.2
*s*1 ($c = 2\,Å^2$)	−28.7 ± 0.5	$2.3 \cdot 10^{-4}$	−40.0 ± 0.4
*s*2 ($c = 0.25\,Å^2$)	−28.8 ± 0.3	$2.5 \cdot 10^{-4}$	−40.1 ± 0.3
*s*3 ($c = 0.04\,Å^2$)	−29.6 ± 0.3	$2.3 \cdot 10^{-4}$	−40.9 ± 0.3
*s*4 ($c = 0.0025\,Å^2$)	−29.9 ± 0.3	$2.4 \cdot 10^{-4}$	−41.2 ± 0.3
*o*12	−29.4 ± 0.1	$-9.3 \cdot 10^{-3}$	−40.7 ± 0.1
*j*12	−30.0 ± 0.1	$6.0 \cdot 10^{-5}$	−41.2 ± 0.1
c	–	$1.4 \cdot 10^{-4}$	–

Simulation	Temperature (K)	cpu time per ps (s)
*o*8	302. ± 2.	365.
*j*8	300. ± 1.	383.
*s*1 ($c = 2\,Å^2$)	301. ± 2.	347.
*s*2 ($c = 0.25\,Å^2$)	301. ± 2.	344.
*s*3 ($c = 0.04\,Å^2$)	300. ± 2.	341.
*s*4 ($c = 0.0025\,Å^2$)	300. ± 2.	347.
*o*12	300. ± 1.	3724.
*j*12	299. ± 1.	3844.
c	–	975.

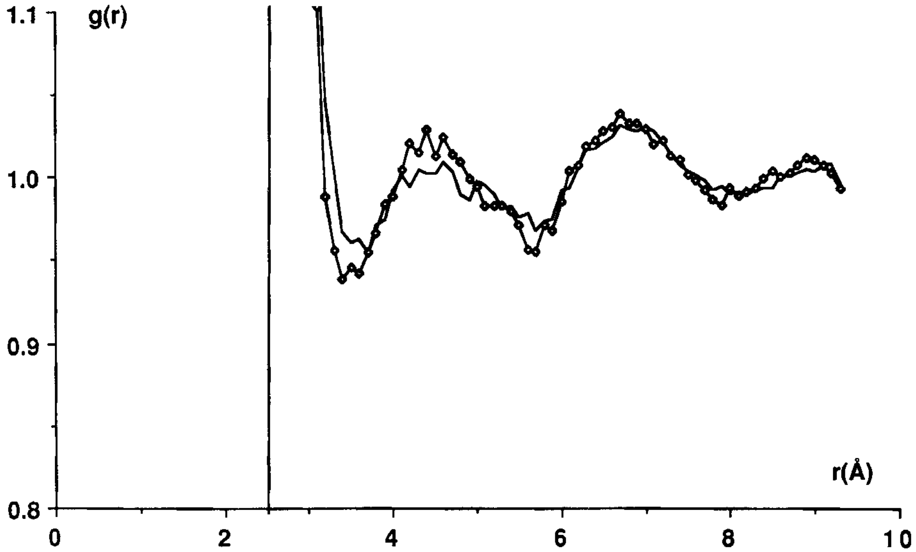

Figure 3 Oxygen to oxygen radial distributions obtained from the *o*8 trajectory (full line) and the *j*8 trajectory (full line with squares).

remains. A buffer zone in the neighbour list would remedy this and reduce drift to the *j*8 level. The energy drift in the cluster simulation was the same as that in the *j*8 trajectory, which indicates that the remaining drift is due to the integration *per se,* and not to the potential discontinuity.

The oxygen–oxygen radial distribution function was found to be insensitive to the potential boundary, a sample comparison is shown in Figure 3. The insensitivity applies also to the oxygen–hydrogen and hydrogen–hydrogen relations, as well as to the O–H bond length and H–O–H bond angle distributions

Translational diffusion coefficients and rotational correlation functions were calculated as in reference [8]. Diffusion coefficients and some rotational correlation times are given in Table 3. The correlation times were obtained from the long time tails, typically 2–10 ps, assuming exponential decay. In some cases the logarithm of the time correlation function was found to be non-linear in the 2–10 ps regime. No correlation time is stated in the table in these cases. To find out whether this is due to further reorientation mechanisms would require substantial amounts of computer time. Unexpectedly, both translational and rotational diffusion seem quite sensitive to the potential boundary. Translation is nearly halved in *j*8 compared to *o*8 and also rotation is retarded. This was the original reason for performing the switching function simulations. With $c = 2\,\text{Å}^2$ (*s*1), the switching function is very gentle and does not cause any large forces. The *s*1 diffusion coefficient is halfway between the *o*8 and *j*8 values. As c is reduced, the switching function gets more abrupt and at $c = 0.0025\,\text{Å}^2$ (*s*4) the switched potential V'_{ij} is indeed close to the unswitched function. The translational diffusion slows down with decreasing c and the *s*4 value is the same as the *j*8 one within statistical uncertainty. This is reasonable, as simulation of the switched potential in the limit of infinite steepness ($c \to 0$, but under such conditions that it takes several time steps to climb the barrier) corresponds to the simulation of the original potential but with the jump correction. The slower dynamics in the *j* simulations may have the following cause. The interaction energy for a pair of molecules inside the neighbour volume is more often negative than not. Thus a molecule attempting to leave experiences, on average, a retaining pull from the jump

Table 3 Dynamic properties. D is the diffusion coefficent obtained from the slope of the mean square displacement as a function of time. τ_l is the rotational correlation time obtained from a single exponential fit to the long time tail (typically 2–10 ps) of the time correlation function C(Δ) of the first order Legendre polynomial of cosθ, where θ is the angle between a vector n at time t and at t + Δ. Vectors used were the dipole moment vector (n_1), a vector perpendicular to the dipole moment but in the plane of the molecule (n_2) and a vector perpendicular to the other two (n_3). Properties were averaged over time and all molecules.

Simulation	*D*		τ_l *(ps)*	
	$(10^{-9} m^2/s)$	n_1	n_2	n_3
*o*8	6.7 ± 0.3	2.0	1.5	1.1
*j*8	3.5 ± 0.2	3.5	2.4	1.9
*s*1 ($c = 2\,\text{Å}^2$)	5.1	2.1	1.8	1.3
*s*2 ($c = 0.25\,\text{Å}^2$)	4.9	2.6	1.8	1.4
*s*3 ($c = 0.04\,\text{Å}^2$)	4.1	2.6	2.2	1.6
*s*4 ($c = 0.0025\,\text{Å}^2$)	3.5	3.6	2.0	1.9
*o*12	6.3	–	1.8	1.4
*j*12	4.7	–	2.1	1.7
c	–	–	–	–

correction, decreasing the probability of the molecule actually leaving. The prolonged neighbour relations then counteract rotation and translation.

The *o*12 and *j*12 simulations were performed to investigate which of the *o*8 and *j*8 trajectories best approximates the dynamics of an infinite system simulated without potential cutoff. When $r_{cut} \rightarrow \infty$ the diffusion coefficient will converge towards the same value in an *o* simulation as in a *j* one. The diffusion coefficient is nearly the same in the *o*12 simulation as in the *o*8, whereas it increases from $3.5 \cdot 10^{-9} m^2/s$ to $4.7 \cdot 10^{-9} m^2/s$ in the *j*12 simulation. This suggests that the diffusion coefficient in a jump corrected simulation may converge to the *o*12 value when r_{cut} becomes large, or, in other words, that the *o*12 value ($6.3 \cdot 10^{-9} m^2/s$) is the more likely guess for the diffusion coefficient when $r_{cut} = \infty$. The same reasoning can be applied to the potential energy, but the conclusion is the other way round. Concomitant to the slower dynamics in the *j* simulations is a lower potential energy. This is the same in the *j*8 and *j*12 trajectories, whereas the *o*12 value is halfway between the *o*8 and the *j*8 ones. Thus, the jump correction technique seems the better choice for static properties (note also the slightly enhanced secondary structure in the radial distribution function of Fig. 3.) whereas the *o* trajectories behave more consistently as regards dynamics. The potential energy in the *s*1 simulation is close to the *o*8 value, while, again, the *s*4-value fully agrees with the *j*8 one.

In conclusion, a dilemma arises. On one hand the original spherical cutoff simulations seem to allow the extraction of dynamic properties from simulations with an economically short potential cutoff, whereas dynamic properties obtained form jump corrected simulations depend on the cutoff distance. On the other hand, the spherical cutoff simulations are mathematically incorrect, as one applies a numerical technique requiring continuous potentials to a model whose discontinuities are quite large. We do not know the relation of the potential and the equation of motion to these trajectories, and there is no stringent indication that they approximate the correct ones. In fact, they do not, as some properties differ from their counterparts obtained from jump corrected simulations. The latter are the correct solutions to the equation of motion for the given potential. Unless a finite range potential is devised, which can be simulated with the stringency of the *j* technique while mimicking dynamics of a long range potential, interpretation of molecular dynamics trajectories for dynamics will continue to require some care.

APPENDIX *SIMULATION PROCEDURE.*

The Newtonian equation of motion was integrated by means of a predictor–corrector two time step algorithm. The predictor was an ordinary Taylor expansion and the corrector used coefficients according to Gear [9]. The two time steps were 0.2 femtoseconds (fs) for bond length and angle forces, and 1.2 fs for dihedral and non-covalent forces. Forces were evaluated from the predicted positions and the difference

$$G_i = \frac{F_i}{m_i} - \frac{d^2 r_{i,p}}{dt^2} \qquad \text{(A1)}$$

was constructed, where *i* is the *x*, *y*, or *z* coordinate of any atom, F_i is the force, $r_{i,p}$ the position and m_i the mass. The final, corrected positions and derivatives $\mathbf{y}_c$ were obtained from the predicted ones $\mathbf{y}_p$ as

$$\mathbf{y}_{\mathrm{i,c}} = \mathbf{y}_{\mathrm{i,p}} + \mathbf{c} \cdot G_{\mathrm{i}} \tag{A2}$$

with

$$\mathbf{y}_{\mathrm{i,p}} = \left(r_{\mathrm{i}}, \frac{dr_{\mathrm{i,p}}}{dt}, \frac{d^2 r_{\mathrm{i,p}}}{dt^2}, \frac{d^3 r_{\mathrm{i,p}}}{dt^3}, \frac{d^4 \mathrm{r}_{\mathrm{i,p}}}{dt^4} \right)^{\mathrm{T}} \tag{A3}$$

and where $\mathbf{c} = (c_0, c_1, c_2, c_3, c_4)^{\mathrm{T}}$ is given in Table A1 for the two time steps. The theory underlying the introduction of two time steps can be found in reference [6].

The potential function has the following form. The hydrogen and oxygen atoms possess point charges which interact according to classical electrostatics. The oxygen atoms also interact with a 6–12 Lennard-Jones potential and the formal expression for the interaction between two sites i and j in two different molecules is

$$u_{\mathrm{ij}}(r_{\mathrm{ij}}) = q_{\mathrm{i}}q_{\mathrm{j}}/(4\pi\varepsilon_0 r_{\mathrm{ij}}) + 4\varepsilon_{\mathrm{ij}}[(\sigma_{\mathrm{ij}}/r_{\mathrm{ij}})^{12} - (\sigma_{\mathrm{ij}}/r_{\mathrm{ij}})^6] \tag{A4}$$,

where $\varepsilon_{\mathrm{ij}} = 0$ when i or j refers to a hydrogen atom. The covalent interactions within a water molecule are treated as harmonic oscillators,

$$u_{\mathrm{intra}}(x) = (k_{\mathrm{e}}/2)(x - x_{\mathrm{e}})^2 \tag{A5}$$

where x is an instantaneous bond length or angle, x_{e} its corresponding gas phase equilibrium value and k_{e} the force constant. All potential parameters are given in Table A2.

Table A1 Gear corrector coefficients

Order	$\Delta t = 0.2\,\mathrm{fs}$	$\Delta = 1.2\,\mathrm{fs}$
c_0	$\frac{19}{6000}\,\mathrm{fs}^2$	$\frac{57}{500}\,\mathrm{fs}^2$
c_1	$\frac{3}{40}\,\mathrm{fs}$	$\frac{9}{20}\,\mathrm{fs}$
c_2	1	1
c_3	$\frac{15}{2}\,\mathrm{fs}^{-1}$	$\frac{5}{4}\,\mathrm{fs}^{-1}$
c_4	$25\,\mathrm{fs}^{-2}$	$\frac{25}{36}\,\mathrm{fs}^{-2}$

Table A2 Interaction parameters for the inter- and intramolecular potential functions. e is the elementary charge.

$q_{\mathrm{O}} = -0.82\,e$	$k_e^{\mathrm{OH}} = 4637\,\mathrm{kJ\ mol^{-1}\,Å^{-2}}$
$q_{\mathrm{H}} = 0.41\,e$	$r_e^{\mathrm{OH}} = 1.0\,\mathrm{Å}$
$\sigma_{\mathrm{OO}} = 3.166\,\mathrm{Å}$	$k_e^{\mathrm{HOH}} = 383\,\mathrm{kJ\ mol^{-1}\,rad^{-2}}$
$\varepsilon_{\mathrm{OO}} = 0.65017\,\mathrm{kJ\,mol^{-1}}$	$\alpha_e^{\mathrm{HOH}} = 109.47°$

Acknowledgement

We thank IBM Corporation for generous allocation of computer time on the IBM 3090-150 VF installed at Lund.

References

[1] F. Lado, "Perturbation Approach to the Computer Simulation of Dipolar Fluids", *J. Chem. Phys.* **85,** 2913 (1986).

[2] V.M. Jansoone, "Dielectric Properties of a Model Fluid with the Monte Carlo Method", *Chem. Phys.* **3,** 78 (1974).

[3] J.A. Barker and R.O. Watts, "Monte Carlo Studies of the Dielectric Properties of Water-like Models" *Mol. Phys.* **26,** 789 (1983).

[4] W.B. Streett, D.J. Tildesley and G. Saville, "Multiple Time Step Methods and an Improved Potential Function for Molecular Dynamics Simulation of Molecular Liquids", *ACS Symp. Ser.* **86,** 144 (1978).

[5] B.R. Brooks, R.E. Bruccoleri, B.D. Olafson, D.J. States, S. Swaminathan and M. Karplus, "CHARMM, a Program for Macromolecular Energy, Minimization and Dynamics Calculations", *J. Comp. Chem.* **4,** 187 (1983), see p. 191.
C.L. Brooks, B.M. Pettitt and M. Karplus, "Structural and Energetic Effects of Truncating Long Ranged Interactions in Ionic and Polar Fluids", *J. Chem. Phys.* **83,** 5897 (1985).

[6] O. Teleman and Bo Jönsson, "Vectorizing a General Purpose Molecular Dynamics Simulation Program", *J. Comp. Chem.* **7,** 58 (1986).

[7] H.J.C. Berendsen, J.P.M. Postma, W.F. van Gunsteren and J. Hermans, "Interaction models for water in Relation to Protein Hydration", in *Intermolecular Forces*, B. Pullman, ed., D. Reidel, 1981, p. 331-342.

[8] O. Teleman, Bo Jönsson and S. Engström, "A molecular Dynamics Simulation of a Water Model with Intramolecular Degrees of Freedom", *Mol. Phys.* **60,** 193 (1987).

[9] C.W. Gear, "*Numerical Initiation Value Problems in Ordinary Differential Equations*" Prentice Hall, Englewood Cliffs, 1971, pp. 148-154.